

DOI 10.24425/ae.2021.136056

Study on the distribution of SAR and temperature in human brain during radio-frequency cosmetic treatment

XINZHE QI, MAI LU^{ORCID}

Key Laboratory of Opt-Electronic Technology and Intelligent Control of Ministry of Education
Lanzhou Jiaotong University
Lanzhou, 730070, Gansu Province, P.R. China
e-mail: mai.lu@hotmail.com

(Received: 03.03.2020, revised: 06.10.2020)

Abstract: This paper established a radio-frequency electrode model and human head model used in RF cosmetic instruments. The distribution of electric field strength, a specific absorption rate (SAR), and temperature distribution in the human brain at 1 MHz and 6 MHz were studied and the results compared with the International Commission on Non-ionizing Radiation Protection (ICNIRP) guidelines. The results showed that under those two frequencies the maximum value of electric field strength in the human brain was 1.52 V/m and it was about 5.4% of the ICNIRP basic restrictions, the maximum SAR in human brain was about 2.21×10^{-3} W/kg, which was far less than 2 W/kg of ICNIRP basic restrictions, the maximum temperature of the human brain was 37.6° located in the wounded skin, which was the same as the normal temperature 37° . Since all the results were within the ICNIRP basic restrictions, the electromagnetic exposure generated by the RF cosmetic electrode will not pose a threat to the human health.

Key words: electromagnetic exposure, human head model, ICNIRP guidelines, radio-frequency cosmetic instruments, safety assessment

1. Introduction

The bio-effects and health risk of radio-frequency (RF) electromagnetic exposure are attracting worldwide attention in recent decades [1, 2]. For the emerging facial rejuvenation technology, RF technology has been widely used in the field of cosmetics. There are many researchers who have studied the safety of radio-frequency technology [3–5], however, most of the studies have focused on whether using different types of radio-frequency electrodes can cause physical damage



© 2021. The Author(s). This is an open-access article distributed under the terms of the Creative Commons Attribution-NonCommercial-NoDerivatives License (CC BY-NC-ND 4.0, <https://creativecommons.org/licenses/by-nc-nd/4.0/>), which permits use, distribution, and reproduction in any medium, provided that the Article is properly cited, the use is non-commercial, and no modifications or adaptations are made.

to the human body. Few studies have been conducted to investigate the electric field strength, a specific absorption rate (SAR) and the distribution of temperature. The RF exposure can lead to bio-effects from nerve and muscle stimulation to thermal injury. The effects to the human central nervous system have been especially studied. The International Commission on Non-ionizing Radiation Protection (ICNIRP) prepared guidelines to prevent the RF heating which potentially has adverse effects on human health [6].

The theory of the RF cosmetic instrument is mainly based on heating the cells in the target area at high temperature to promote the regeneration of tissue cells. When the electrode is applied to the human tissue, an electric field is generated between the electrode and the skin. Since the human tissue can be considered as the electrical conductor, during the application of RF electric field, the water molecules in the tissue will be rotated and moved back and forth instantly. During this vibration process, the molecules touch each other or touch the surrounding medium. This process generates heat which acts on the target tissues. The heat makes collagen shrinking and tightening, which allows the natural healing of the human tissue, and as a result, the skin is tightened [7].

The rate of healing collagen depends on the time and temperature, if the temperature of skin is high enough, the exposure time will be shorter. At 85°C, an exposure time of about 1 ms is sufficient to cause structural changes in collagen [8]. But higher temperatures increase the likelihood of burns or other adverse effects. According to the Arrhenius equation, lower temperatures can be used to reduce risk, but this requires a longer heating time [9]. Usually there are 2 phases [10], phase 1 is non-therapeutic, the goal of phase 1 is to elevate the temperature to 39°C; phase 2 is a therapeutic phase, the goal of phase 2 is to increase the temperature to the target temperature.

The composition of the radio-frequency cosmetic instrument includes five parts: a radio-frequency circuit, a power amplifier unit, a control unit, an electrode and a power supply system. The radio-frequency circuit generates current and transmits it to the electrode after passing through the power amplifier. In the simulation, the lower surface of the electrode is used as the power output terminal, and this port is defined as 40 W. The electrode simulated in this paper was a fractional radio-frequency electrode. The electrodes are covered with micro-needles arranged in pairs, and current is transmitted between two adjacent needles. Each pair of electrodes is grounded to form a bipolar RF instrument.

Because of human ethics issues, it is impossible to directly measure the electric field strength, SAR and temperature fields in the human tissue. The ideal way is to perform numerical calculations to get the electromagnetic field distribution in the human tissue. This study selected two commonly used frequencies in radio-frequency cosmetic instruments: 1 MHz [11] and 6 MHz [12] to study the electric field strength, SAR and temperature distribution in the human brain while people are receiving radio-frequency treatments. To assess the safety of radio-frequency cosmetic technology, the obtained electric field strength and SAR were compared with ICNIRP guidelines.

2. Theory and model

2.1. Theory

A SAR is defined as:

$$\text{SAR} = \frac{\sigma}{\rho} E^2, \quad (1)$$

where: σ is the conductivity (S/m), ρ is the mass density (kg/m^3), \mathbf{E} is the electric field strength (V/m). So, first, we need to calculate the electric field strength. The calculation of the electric field strength is according to Maxwell's equations:

$$\nabla \times \mathbf{H} = \mathbf{J} + \frac{\partial \mathbf{D}}{\partial t}, \quad (2)$$

$$\nabla \times \mathbf{E} = -\frac{\partial \mathbf{B}}{\partial t}, \quad (3)$$

$$\nabla \times \mathbf{D} = \rho, \quad (4)$$

$$\nabla \times \mathbf{B} = 0, \quad (5)$$

where: \mathbf{H} is the magnetic field strength (A/m), \mathbf{J} is the current density (A/m^2), \mathbf{D} is the electric flux (C/m^2), \mathbf{E} is the electric field strength (V/m), \mathbf{B} is the magnetic induction (T), ρ is the charge density (C/m^3), and three additional equations are:

$$\mathbf{D} = \varepsilon \mathbf{E}, \quad (6)$$

$$\mathbf{B} = \mu \mathbf{H}, \quad (7)$$

$$\mathbf{J} = \sigma \mathbf{E}, \quad (8)$$

where: ε , μ , σ , stand for the permittivity (F/m), magnetic permeability (H/m) and conductivity (S/m), respectively.

Considering the concept of hemoperfusion [11], the bioheat equation governs heating during the treatment:

$$\rho c \frac{\partial T}{\partial t} = k \nabla^2 T + \rho_b c_b \omega_b (T_b - T) + P, \quad (9)$$

where: ρ (kg/m^3), c ($\text{J/kg}\cdot\text{K}$), k ($\text{W/m}\cdot\text{K}$) are the density, heat capacity and thermal conductivity. T_b is the blood temperature, ρ_b (kg/m^3), c_b ($\text{J/kg}\cdot\text{K}$) are the blood density and heat capacity. ω_b (1/s) is the blood perfusion, P is the Joule heat, generated by the electromagnetic field as an external heat source.

2.2. Establishment of finite element mode

In order to simulate the distribution of RF electromagnetic fields in the human brain, a five-sphere human head model has been established. It consists of three parts: the scalp, the skull and the brain. The scalp and skull are composed of 92 mm and 85 mm spheres [13], the cerebrospinal fluid (CSF) is composed of 80 mm spheres, the brain gray matter is composed of 78.8 mm spheres, and the white matter of the brain is composed of 75.8 mm spheres. However, since an RF electrode is applied to human skin, the skin should be modeled more meticulously. Human skin is divided into several layers. The skin is divided into stratum corneum (SC), epidermis/dermis (E/D) and hypodermis (HYP) [16], and the wounded skin is located in the E/D [17], as for the thickness, the SC is 0.02 mm, the E/D is 1.43 mm, the HYP is 5 mm and the wounded skin is 1.2 mm thick [18]. The head model is shown in Fig. 1(a), in the head model, the space between layers of the skin tissue was thin, so the mesh of different kinds of tissue was different, the mesh is shown in Fig. 1(b). Fig. 2 shows the layered skin model.

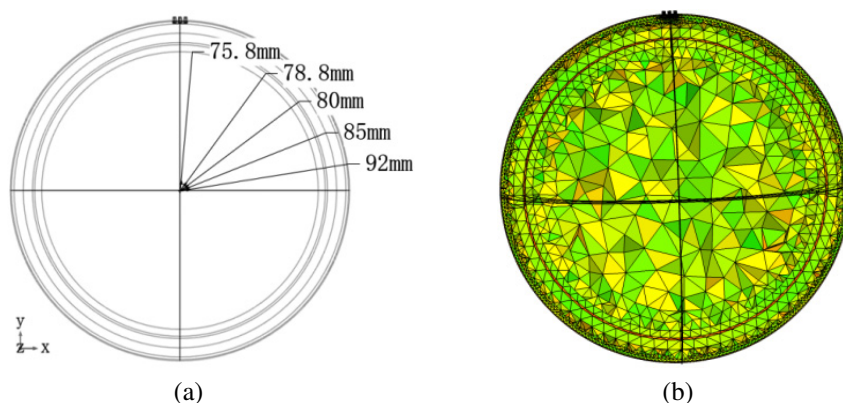


Fig. 1. Head model: cross section of head model (a); 3D head meshing (b)

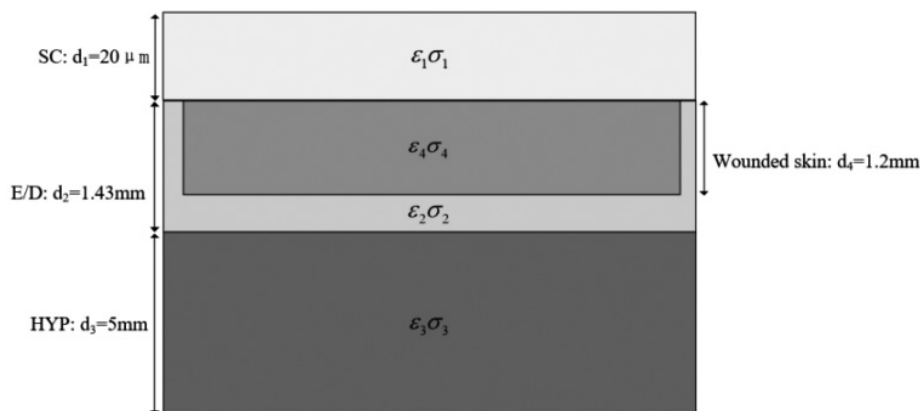


Fig. 2. Cross-section of skin tissue

The dielectric parameter for head tissues is calculated by the 4-Cole-Cole model [18]. Assume that the medium of each part of the head tissue is evenly distributed, the dielectric parameters at 1 MHz and 6 MHz are illustrated in Table 1, the heat parameters are illustrated in Table 2 [21]. The initial temperature in the human head is 37°C.

The radio-frequency electrode, which has been widely used, was described in this paper. The material of the electrode is medical 430 stainless steel, every little electrode tip is a cone-shape with a bottom surface radius of 0.8 mm and a height of 3 mm, the distance between the electrode tips is 1 mm. The electrode tips are located in the wounded skin. The power of 40 W is used in the simulation, and the electrode model is shown in Fig. 3.

COMSOL Multiphysics is advanced multi-physical field numerical simulation software based on the finite element method, which archives real physical phenomena by solving partial differential equations [22]. It is widely used in engineering calculation, scientific research, simulation science and other fields. The simulation conducted in this study was based on the version of

Table 1. Dielectric parameters at 1 MHz and 6 MHz

Human tissue	Permittivity (F/m) (1 MHz)	Conductivity (S/m) (1 MHz)	Permittivity (F/m) (6 MHz)	Conductivity (S/m) (6 MHz)
White matter	479.79	0.10	216.34	0.14
Gray matter	860.42	0.16	421.8	0.24
CSF	108.99	2.00	108.85	2.00
Skull	144.51	0.024	51.84	0.038
HYP	27.2	0.025	17.11	0.027
E/D	3026.3	0.82	483.57	1.06
SC	904.2	0.10	220.6	0.21
Wounded skin	990.76	0.013	518.3	0.13

Table 2. Heat parameters of human tissue

Human tissue	Heat capacity (J/(kg·K))	Thermal conductivity (W/(m·K))	Blood perfusion (1/s)	Density (kg/m ³)
White matter	3582.8	0.48	1552	1041
Gray matter	3695.8	0.50	1500	1044.5
CSF	4095.5	0.57	1504	1077
Skull	2300	1.16	2117	1500
Skin	3391	0.37	1624	1109

COMSOL Multiphysics 5.4, the calculation space was meshed into 725 766 elements. The computer with 4 cores, 16 GB ram was used in the calculations. The calculation time was 30 minutes for each simulation.

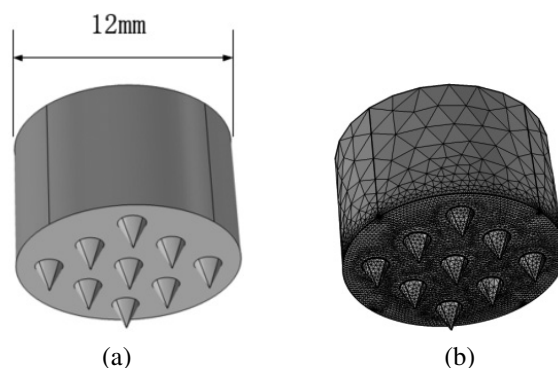


Fig. 3. Electrode model: 3D electrode model (a); electrode meshing (b)

2.3. ICNIRP guidelines

Since the human body is a lossy dielectric media, exposure to RF electromagnetic fields can lead to significant absorption of energy and temperature increases. To avoid potentially adverse health effects, the International Commission on Non-Ionizing Radiation Protection (ICNIRP) has defined reference levels for time varying magnetic fields [6]. RF exposure may produce heating in the human body which can be measured by a specific absorption rate (SAR). ICNIRP guidelines have set limits for both public and occupational exposures for different frequencies. As for the frequencies of this study, the limits are shown in Table 3.

Table 3. INCIRP basic restrictions (1 MHz–10 MHz)

	E (V/m)	SAR (head and trunk) (W/kg)	SAR (whole-body average) (W/kg)
Public exposure	$610/f$	2	0.08
Occupational exposure	$87/f^{1/2}$	10	0.4

3. Simulation results and analysis

3.1. Distribution electric fields in the brain

In order to study the distribution of the electric field in the human brain, a slice of the longitudinal section of the head in the XY plane was selected, the slice is perpendicular to the electrode, and the distribution of the electric field vector in the longitudinal slice of the head is shown in Fig. 4. The electric field vector distribution is in a symmetrical manner. The maximum electric field was on the skin located under the bottom of the electrode.

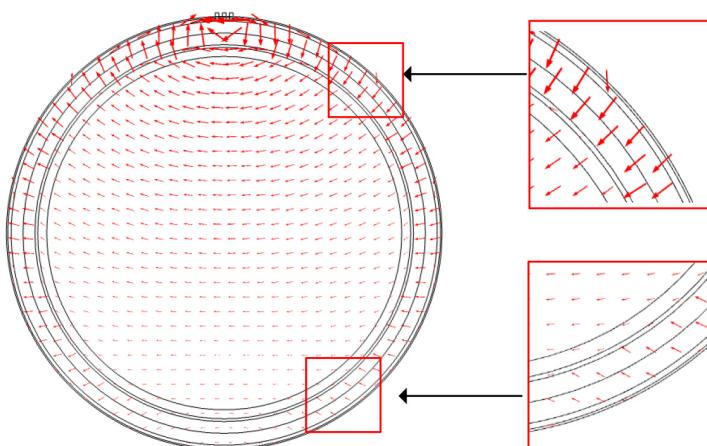


Fig. 4. E distribution in the slice of head model

The electric field distribution in the central nervous system is important during radio-frequency cosmetology. Therefore, a section of the wounded skin, gray matter and white matter was taken under the electrode inside the human head. The section under the electrode was located at $y_1 = 90.5$ mm, and this section was inside the wounded skin tissue. The gray matter section was located at $y_2 = 77$ mm and the white matter section was located at $y_3 = 65$ mm. All of the three sections were in the XY plane, and the results were shown in Fig. 5 and Fig. 6, respectively.

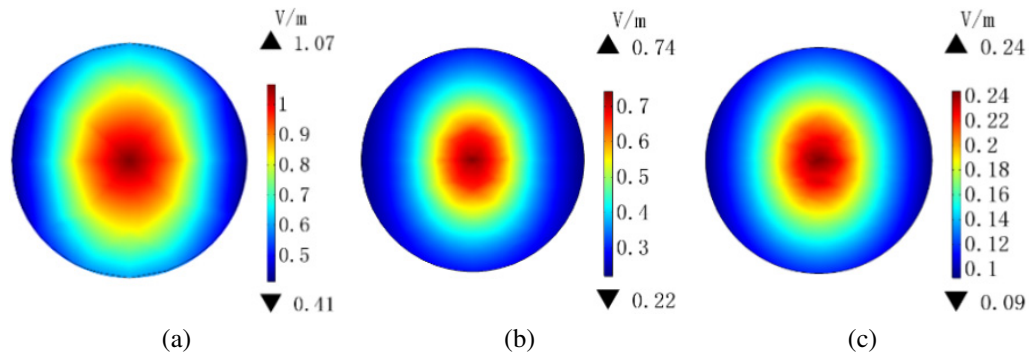


Fig. 5. E -field distribution in the slice of brain (1 MHz): underneath the electrode (a); gray matter (b) and white matter (c)

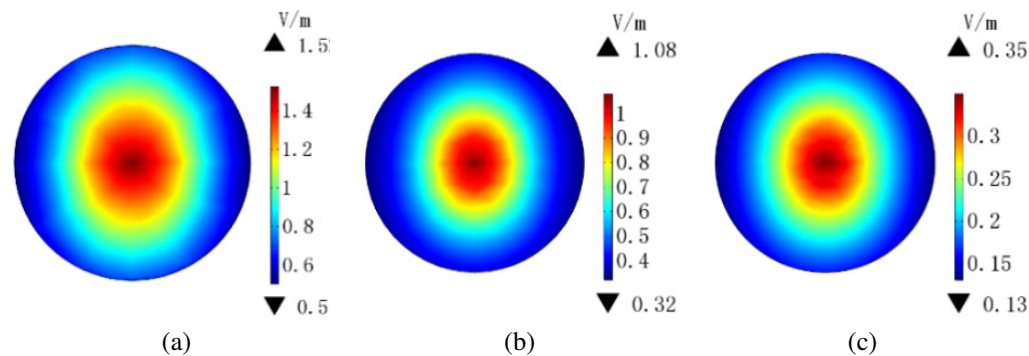


Fig. 6. E field distribution in the slice of brain (6 MHz): underneath the electrode (a); gray matter (b) and white matter (c)

From the results one can find that the E -field with the maximum value occurred in the wounded tissues under the electrode. The E -field was decreased with the increased depth in the tissue. For the frequency of 1 MHz, the maximum of E -field was 1.07 V/m which was about 3.8% of the ICNIRP limits. In the brain tissues, the maximum of E -field in the gray matter and white matter was 0.74 V/m and 0.24 V/m, respectively, both values were under the ICNIRP limits. The electric field underneath the electrode can be 76.9% higher than that in the white matter of the brain. For a frequency of 6 MHz, the maximum of E -field was 1.52 V/m which was about 5.4% of the ICNIRP limits. In the brain tissues, the maximum of E -field in the gray matter and white

matter was 1.08 V/m and 0.35 V/m, respectively. Both values were under the ICNIRP limits. The electric field underneath the electrode can be 76.9% higher than that in the white matter of brain.

In the same tissue, when different frequencies were used, it can be seen that the electric field intensity increased with the increase of frequency, and the distribution of electric field intensity in all parts was consistent, the largest value was presented in the center of the slice, and it decreased with the increased distance from the center.

3.2. SAR distribution in brain

The same slices underneath the electrode were employed to study the distribution of the SAR in gray matter and white matter, as shown in Fig. 7 and Fig. 8, respectively. From the results one can find that the SAR with the maximum value was presented in the wounded tissues under the electrode. The SAR was decreased with the increased depth in tissues. For a frequency of 1 MHz, the maximum of SAR was 1.08×10^{-3} W/kg, less than the ICNIRP limits. In the brain tissues, the maximum values of the SAR in the gray matter and white matter were 3.42×10^{-5} W/kg and 2.85×10^{-6} W/kg, respectively, both values were under the ICNIRP limits. The SAR underneath the electrode can be 99.7% higher than that in the white matter of brain. For a frequency of 6 MHz, the maximum of SAR was 2.21×10^{-3} W/kg. In the brain tissues, the maximum SARs in the gray matter and white matter were 1.37×10^{-4} W/kg and 8.43×10^{-5} W/kg, respectively, both values were under the ICNIRP limits. The SAR underneath the electrode can be 99.6% higher than that in the white matter of the brain.

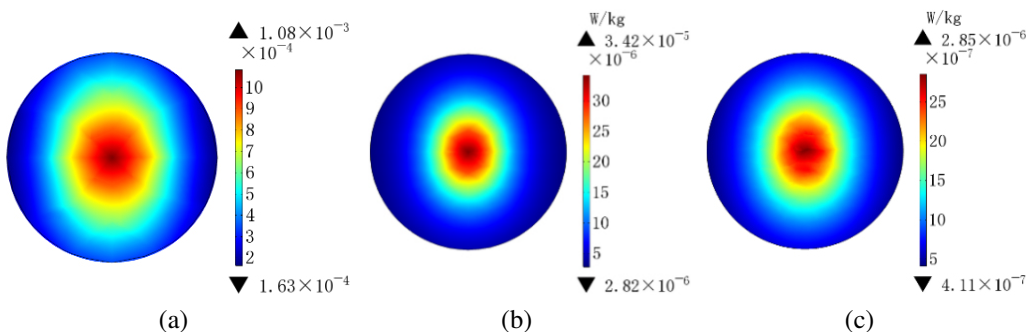


Fig. 7. The SAR distribution in the slice of brain (1 MHz): underneath the electrode (a); gray matter (b); white matter (c)

It was observed with the increase of frequency, the SAR was constantly increasing, which was consistent with the change of the electric field. This is because, as can be seen from Equation (1), the SAR was in proportion to the electric field intensity. The SAR value in the head center was the largest and gradually decreased with the increase of the distance from the center. The SAR underneath the electrode at 6 MHz was 51.1% larger than that of 1 MHz. The SAR at 6 MHz in the gray matter was about 75% larger than that of 1 MHz, and the SAR at 6 MHz in the white matter was about 66.1% larger than that of 1 MHz.

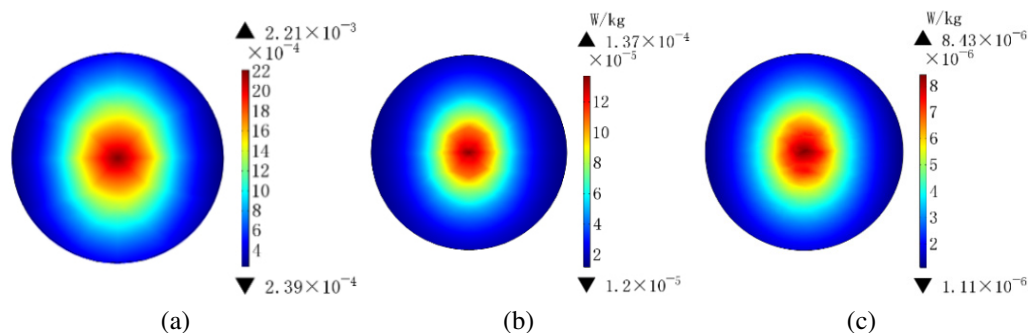


Fig. 8. The SAR distribution in the slice of brain (6 MHz): underneath the electrode (a); gray matter (b); white matter (c)

3.3. Temperature distribution in brain

The principle of radio-frequency cosmetic instruments is that high temperature kills cells in the target area and promotes cell regeneration. In actual clinical applications, it is often necessary to apply gel to the place where the electrode is in contact with skin to cool down the temperature and to increase the conductivity. The temperature distribution on the surface of the skin has been photographed by thermal imaging cameras [8, 9]. However, the temperature distribution in the human body is still not clear. According to ICNIRP guidelines, exposure to high-frequency electromagnetic causes that the temperature of the human body increases, causing the potential damage to the nervous system because of thermal effects. Since the human cells die gradually at 42°C, it is necessary to study the temperature inside the brain to further evaluate the safety of radio-frequency cosmetic instruments. To achieve this goal, the temperature distributions in typical slices i.e. under the electrode ($y_1 = 90.5$ mm), on the surface of the skull ($y_4 = 84$ mm), in the cerebrospinal fluid ($y_5 = 79$ mm), in the gray matter ($y_2 = 77$ mm) and in the white matter ($y_3 = 63.5$ mm) were analyzed. The 1 MHz calculation results are shown in Fig. 9, and 6 MHz calculation results are shown in Fig. 10.

The results showed that under the electrode, the temperature reached 43.6°C at 1 MHz. At this temperature, water in cells evaporates, the cells shrink and become necrotic which promotes the regeneration of collagen. Thus, the purpose of radio-frequency therapy was achieved. The temperature in this part was relatively well distributed, the temperature at the center was the largest, and the temperature gradually decreased from the center to the periphery. In the non-therapeutics area, the temperature was maintained at about 37°C. This kind of distribution avoided damage to non-therapeutics areas, allowing energy to be concentrated on the wounded skin.

But due to the different dielectric properties of human tissue, the temperature in the head decreased quickly, the temperature reached 38.5°C at 1 MHz and 40.7°C at 6 MHz, respectively. The temperature was still higher than human normal temperature 37°C, but it no longer caused damage to the cells, so it is safe for humans. The temperature distribution in this part was similar to that in the section under the electrode, the temperature was relatively centralized and the temperature in the center was the highest, but the temperature in the surrounding tissue decreased rapidly. Generally speaking, the temperature in this part will not cause damage to the human body.

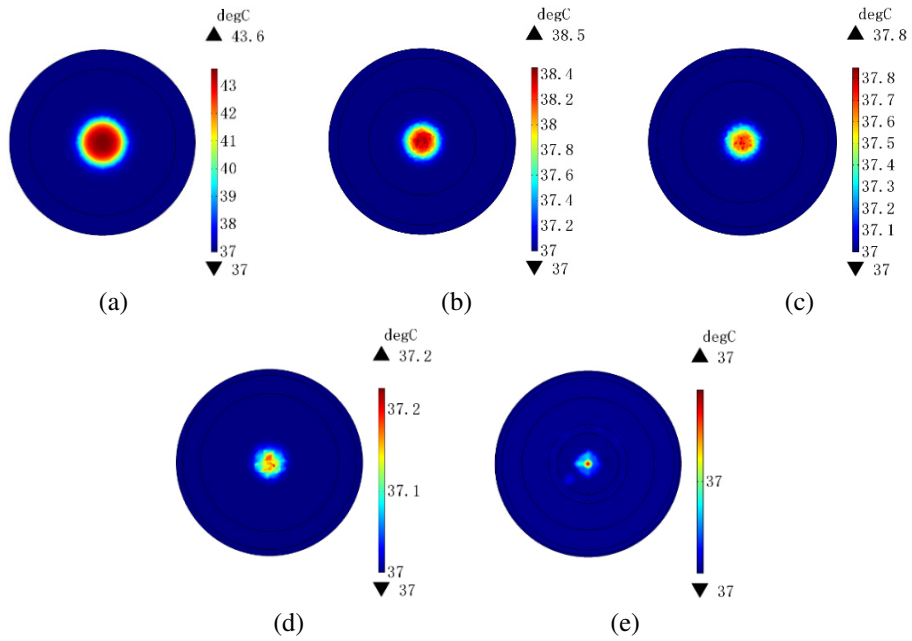


Fig. 9. Temperature distribution at 1 MHz: underneath the electrode (a); the surface of the skull (b); cerebrospinal fluid (c); gray matter (d); white matter (e)

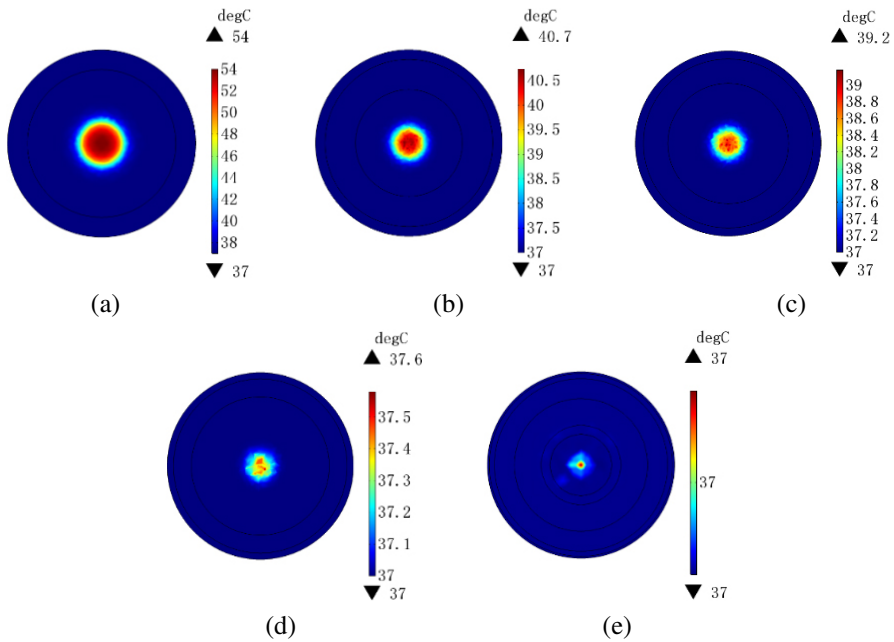


Fig. 10. Temperature distribution at 6 MHz: underneath the electrode (a); the surface of the skull (b); cerebrospinal fluid (c); gray matter (d); white matter (e)

Take the cerebrospinal fluid for example, the temperature in CSF was 37.8°C at 1 MHz, which was close to human normal temperature, and the temperature was 39.2°C at 6 MHz, the temperature difference between the two frequencies was 1.4°C. But in the gray matter, the temperature was 37.2°C at 1 MHz and 37.6°C at 6 MHz, the difference between the two frequencies was 0.4°C, which means the cerebrospinal fluid reduced the temperature by absorbing heat.

It was found that with the increase of frequency, the temperature in the tissues also increased. The closer to the electrode, the greater the temperature change. However, for different frequencies, the temperature distribution in the tissues was similar.

4. Conclusions

This research mainly studied the distribution of an electric field, SAR and temperature in human heads (especially the central nervous system) generated by a radio-frequency electrode used in radio-frequency cosmetic instruments at 1 MHz and 6 MHz, and assessed the safety of the electromagnetic exposure. The conclusions are as follows.

The value of the SAR increased with the increase of frequency, the maximum of the SAR at two frequencies was 2.21×10^{-3} W/kg and it was about 0.11% of the ICNIRP basic restrictions, the SAR at 6 MHz was 51.1% larger than that at 1 MHz underneath the electrode. At the same frequency, the SAR value decreased with the increased depth, and the attenuation was fast. The maximum SAR was under the electrode, and the SAR in the white matter area would be reduced by at least two orders of magnitude.

The temperature gradually increased with the increase of frequency. The highest temperature in the gray matter at two frequencies inside the brain was 37.2°C, which indicated that the temperature gradually decreased with the increased depth of the head tissues. Due to the endothermic effect of cerebrospinal fluid, the temperature of the brain tissue has been consistent with the normal body temperature of the human body. At the same location, as the depth increased, the temperature difference at different frequencies was gradually smaller. At the same frequency, the temperature distribution was more consistent and gradually decreased with the depth of the head tissues, the temperature difference between the electrode and the white matter was 31.4%.

Research showed that the electric field strength and SAR in the brain were below the ICNIRP guidelines, and the temperature was the same as the normal human body temperature, which indicated that the electromagnetic field generated by the radio-frequency cosmetic instruments will not cause damage to the human body. However, the temperature under the electrode was a little bit higher and it may cause damage to the surrounding tissue. So, in practical application methods, objectives such as reducing treatment time or enhancing cooling measurements should be further investigated to prevent the damage caused by increased temperature. The results of this study reveal the safety of radio-frequency cosmetic instruments, but there are still some shortcomings. For example, this paper only modeled dry skin. Since the dielectric properties of dry skin and wet skin are different, the distribution of the SAR and temperature in wet skin might be different.

Acknowledgements

This research was financially supported by the National Natural Science Foundation of China (grant nos. 51567015, 51867014), and by the Department of Education of Gansu Province under Grant 2018D-08.

References

- [1] Bidi M., *Biological risk assessment of high-voltage transmission lines on worker's health of electric society*, Archives of Electrical Engineering, vol. 69, no. 1, pp. 57–68 (2020).
- [2] Deltuva R., Lukočius R., *Electric and magnetic field of different transpositions of overhead power line*, Archives of Electrical Engineering, vol. 66, no. 3, pp. 595–605 (2017).
- [3] Alam M., Levy R., Pajvani U., Ramirez A., Guitart J., Veen H., Gladstone B., *Safety of radiofrequency treatment over human skin previously injected with medium-term injectable soft-tissue augmentation materials: a controlled pilot trial*, Lasers in Surgery and Medicine, vol. 39, no. 5, pp. 468–468 (2007).
- [4] Suh D.H., Byun J.E., Lee J.S., Song Y.K., Kim S.H., *Clinical efficacy and safety evaluation of a novel fractional unipolar radiofrequency device on facial tightening: A preliminary report*, Journal of Cosmetic Dermatology, vol. 16, no. 2, pp. 199–204 (2017).
- [5] Lee S.H., Lee D.H., Won C.H., Chang H.W., Kwon H.H., Kim K.H., Chung J.H., *Fractional rejuvenation using a novel bipolar radiofrequency system in Asian skin*, Dermatol Surgery, vol. 37, no. 11, pp. 1611–1619 (2011).
- [6] *International Commission on Non-ionizing Radiation Protection Guidelines for limiting exposure to time-varying electric and magnetic fields (up to 300GHz)*, Health Physics, vol. 74, no. 4, pp. 494–522 (1998).
- [7] Alhalabi S.M., Agha O.Q., Hantash B.M., *Nonablative radiofrequency for skin rejuvenation: a review of the literature*, Expert Review of Dermatology, vol. 7, no. 7, pp. 589–599 (2012).
- [8] Sadick N., *Tissue tightening technologies: Fact or fiction*, Aesthetic Surgery Journal, vol. 28, no. 2, pp. 180–188 (2008).
- [9] Nelson A., Beynet D., Lask G., *A novel non-invasive radiofrequency dermal heating device for skin tightening of the face and neck*, Journal of Cosmetic and Laser Therapy, vol. 17, no. 6, pp. 1–6 (2015).
- [10] Friedman J., Gilead L., *The Use of Hybrid Radiofrequency Device for the Treatment of Rhytids and Lax Skin*, Dermatologic Surgery, vol. 33, no. 5, pp. 547–551 (2007).
- [11] Brightman L., Goldman MP., Taub A.F., *Sublative Rejuvenation: Experience with a New Fractional Radiofrequency System for Skin Rejuvenation and Repair*, Journal of Drugs in Dermatology, vol. 8, no. 11, pp. 9–13 (2009).
- [12] Hsu T.S., Kaminer M.S., *The use of nonablative radiofrequency technology to tighten the lower face and neck*, Seminars in Cutaneous Medicine and Surgery, vol. 22, no. 2, pp. 1–123 (2003).
- [13] Rush S., Driscoll D.A., *EEG electrode sensitivity—an application of reciprocity*, IEEE Transactions on Biomedical Engineering, vol. 16, no. 1, pp. 15–22 (1968).
- [14] Huclova S., Baumann D., Talary M., Frohlich J., *Sensitivity and specificity analysis of fringing-field dielectric spectroscopy applied to a multi-layer system modelling the human skin*, Physics in Medicine and Biology, vol. 56, no. 24, pp. 7777–7793 (2011).
- [15] Gabriel C., Bentall R., Grant E.H., *Comparison of the dielectric properties of normal and wounded human skin material*, Bioelectromagnetics, vol. 8, no. 1, pp. 23–27 (1987).
- [16] Huclova S., Erni D., Frohlich J., *Modelling and validation of dielectric properties of human skin in the MHz region focusing on skin layer morphology and material composition*, Journal of Physics D Applied Physics, vol. 45, no. 45 (2012), DOI: [10.1088/0022-3727/45/2/025301](https://doi.org/10.1088/0022-3727/45/2/025301).

- [17] Cole K., Cole R., *Dispersion and absorption in dielectrics: I. Alternating current characteristics*, Journal of Chemical Physics, vol. 9, no. 4, pp. 341–351 (1941).
- [18] <http://www.itis.ethz.ch/database.pl>, accessed January 2020.
- [19] <http://cn.comsol.com/pl>, accessed January 2020.
- [20] Rush S., Driscoll D.A., *Current distribution in the brain from surface electrodes*, Anesthesia and Analgesia, vol. 47, no. 6, pp. 717–723 (1968).
- [21] Tamnes K., Ostby Y., Fjell A.M., Westlye L.T., Due P., Walhovd K., *Brain maturation in adolescence and young adulthood: regional age-related changes in cortical thickness and white matter volume and microstructure*, Cerebral Cortex, vol. 20, no. 3, pp. 534–548 (2010).
- [22] Gabriel S., Lau W., Gabriel C., *The dielectric properties of biological tissues: III parametric models for the dielectric spectrum of tissues*, Physics in Medicine and Biology, vol. 41, no. 11, pp. 2271–2293 (1996).
- [23] Hruza G., Taub F., Collier S., Mulholland R., *Skin rejuvenation and wrinkle reduction using a fractional radiofrequency system*, Journal of Drugs in Dermatology, vol. 8, no. 3, pp. 259–265 (2009).